1,1-Dicyano-2-[6-(dimethylamino)naphthalen-2-yl]propene (DDNP): A Solvent Polarity and Viscosity Sensitive Fluorophore for Fluorescence Microscopy[⊥]

A. Jacobson,[§] A. Petric,[‡] D. Hogenkamp,[§] A. Sinur,[†] and J. R. Barrio*[,§]

Contribution from the Department of Molecular and Medical Pharmacology and the Laboratory of Structural Biology and Molecular Medicine, UCLA School of Medicine, Los Angeles, California 90095-6948, Faculty of Chemistry and Chemical Technology, University of Ljubljana, 6100 Ljubljana, Slovenia

Received December 29, 1995[⊗]

Abstract: 1,1-Dicyano-2-[6-(dimethylamino)naphthalen-2-yl]propene (**II**, DDNP) has been synthesized as a fluorescent dye whose intramolecular rotational relaxation is solvent polarity and viscosity dependent. Its fluorescence emission (λ max: 470−610 nm in hydrophobic and viscous environments) is in a very favorable region for its use with visible fluorescence microscopy, without interference from cell or tissue autofluorescence. Its fluorescence emission quantum yield in an aqueous environment is very low, allowing for facile differentiation between lipid or protein bound state and aqueous media. **II** crystallizes into two solid isoforms containing one (red crystals) and two conformers (yellow crystals), exhibiting differing spectral properties. X-ray crystal structures reveal a planar arrangement between dimethylamino and naphthalenyl moieties, with out-of-plane arrangements between the malononitrile and naphthalene ring found in each of the three conformers.

Introduction

Environmentally sensitive fluorescence, by virtue of varying responses to solvent media, provides a wealth of information on the physical and chemical properties of molecular microenvironments. Fluorophores that are electronically interactive with solvents or other solute molecules are fluorescent chemosensors,[1] sensitive to an array of factors, such as ions,[2] environmental rigidity,[3] or electric polarization in cell membranes.[4] The range of experiments in which environmentally sensitive fluorophores can be used, however, is limited by the wavelength ranges in which useful environmental sensitivity can be found. Although a number of these fluorophores are used in biological assays (i.e., 2-acyl-6-dimethylaminonaphthalene derivatives, like ADMAN (I) and PRODAN),[5,6] few polarity or viscosity sensitive probes are available with absorption in the wavelength range around 420 nm, below which significant autofluorescence occurs in many biological systems.

In this work we report the development of a novel fluorophore with excitation in nonaqueous solvents or rigid media centered at 430−440 nm and emissions at 470−610 nm, with excellent properties for visible wavelength fluorescence microscopy using standard argon, argon/krypton laser illumination, or conventional lamp sources. The compound, 1,1-dicyano-2-[(6-dimethylamino)naphthalen-2-yl]propene (DDNP) (**II**) (Chart 1), demonstrates solvent polarity dependent changes in excitation and emission wavelengths and viscosity dependent changes in quantum yield. Its environmental sensitivity shows characteristics of an excited state charge transfer (CT) complex.[7−12] Recently fluorophores structurally related to *trans*-stilbenes, 4-*p*-dimethylaminostyrylpyridinium salts, were reported to be sensitive to temperature and viscosity in protic solvents.[13] These derivatives are charged fluorophores with dual fluorescence in the visible regions and a low energy twisted intramolecular charge transfer (TICT) band sensitive to viscosity.

Chart 1

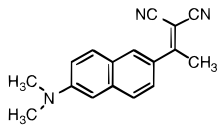

II

DDNP crystallizes into at least two solid isoforms exhibiting markedly different absorption and fluorescence emission spectra. X-ray crystallographic data are also presented to correlate the putative molecular conformations of the two forms with their spectroscopic properties. The details of this investigation are presented herein.

Experimental Section

Heptadecane and mineral oils were obtained from Aldrich (Milwaukee, WI). Poly(ethylene)glycols were purchased from Serva (Paramus, NJ). Deionized water was used for the preparation of solutions (Millipore RO system). Bovine serum albumin (BSA) was procured

* To whom correspondence should be addressed: Department of Molecular and Medical Pharmacology, B2-086A Center for the Health Sciences, Los Angeles, CA 90095-6948.
† University of Ljubljana.
‡ On leave from the University of Ljubljana, Ljubljana, Slovenia.
§ UCLA School of Medicine.
⊥ Key words: fluorescence/environmental sensitivity/conformers.
⊗ Abstract published in *Advance ACS Abstracts,* June 1, 1996.

(1) Czarnik, A. W. *Acc. Chem. Res.* **1994**, *27*, 302−308.
(2) Tsien, R. Y. *Ann. Rev. Neurosci.* **1989**, *12*, 227−253.
(3) Loutfy, R. O. *Macromolecules* **1981**, *14*, 270−275.
(4) Loew, L. M.; Simpson, L. L. *Biophys. J.* **1981**, *34*, 353.
(5) Weber, G.; Farris, F. J. *Biochemistry* **1979**, *18*, 3075−3078.
(6) Macgregor, R. B.; Weber, G. *Nature* **1986**, *319*, 70−73.
(7) Loutfy, R. O.; Law, K. Y. *J. Phys. Chem.* **1980**, *84*, 2803−2808.
(8) Rollinson, A. M.; Drickamer, H. G. *J. Chem. Phys.* **1980**, *73*, 5981−5996.
(9) Nowak, W.; Adamczak, P.; Balter, A.; Sygula, A. *J. Mol. Struct. (Theochem.)* **1986**, *139*, 13−23.
(10) Rettig, W. *Angew. Chem., Int. Ed. Engl.* **1986**, *25*, 971−988.
(11) Heisel, F.; Miehe, J. A.; Szemik, A. W. *Chem. Phys. Lett.* **1987**, *138*, 321−326.
(12) Balter, A.; Nowak, W.; Pawelkiewicz, W.; Kowalczyk, A. *Chem. Phys. Lett.* **1988**, *143*, 565−570.
(13) Wandelt, B.; Turkewitsch, P.; Stranix, B. R.; Darling, G. D. *J. Chem. Soc., Faraday Trans.* **1995**, *91*, 4199−4205.

S0002-7863(95)04335-6 CCC: $12.00

from Sigma (St. Louis, MO). Other solvents used were spectroscopic grade or better and were obtained from Fisher (Tustin, CA). All solvents were degassed and sparged with argon prior to use. Absorption spectra were determined at concentrations around 2×10^{-5} M with a Beckman DU-50 spectrophotometer. NMR and IR spectra were recorded on a Bruker AM-360WB spectrometer and a Perkin-Elmer 710B IR spectrophotometer, respectively. Fluorescence spectra were determined on SLM 4800C (ADMAN, DDNP) and Perkin-Elmer LS-50B (DDNP) fluorescence spectrophotometers, with slit widths routinely set at 4−5 nm. For DDNP measurements, both standard and red sensitive (R-928) photomultiplier tubes were used. Fluorescence was referenced to solvent blank using matched cells (Spectrocell, Inc), with emission corrected for photomultiplier wavelength response. Quantum yields (Q) were determined relative to quinine sulfate in 0.1 N H_2SO_4 (Regis Chemicals, Morton Grove, IL) ($Q = 0.55$, excitation = 365 nm)[14,15] or Rhodamine 101 (Kodak, Rochester NY) ($Q = 0.97-1$; excitation = 393−460 nm).[16−18] Melting points were determined on an electrothermal melting point apparatus and are uncorrected. HPLC conditions for analysis of **II** were as follows: Reverse phase Econosil C-18 column 5 μm, 250 × 4.6 mm. Solvent: H_2O:CH_3CN, 7:13, with detection by UV absorption at 360 nm. Elemental analyses were performed by Galbraith Laboratories, Inc., Knoxville, TN.

X-ray Structure Determination. X-ray crystallographic data were obtained on the two solid isoforms of DDNP, A (red needles) and B (yellow plates). Crystals of both isoforms were grown from benzene solution under petroleum ether (30−60°) vapor. For isoform (A): monoclinic, $P2_1/n$, no. 14, $a = 4.031(1)$, $b = 13.269$ (3), $c = 26.030$ (7) Å, $\beta = 93.63(2)°$, $V = 1389.5(6)$ Å^3, $Z = 4$, $D_x = 1.249$ Mg/m^3, $D_m = 1.24(2)$ Mg/m^3, Mo Kα radiation, $\lambda = 0.71069$ Å, $\mu = 0.07075$ mm^{-1}, $T = 293$ (2) K, crystal shape: needle, crystal size: 0.08 mm × 0.20 mm × 0.44 mm. For isoform (B): monoclinic, $P2_1/n$, no. 14, $a = 17.668(5)$, $b = 7.627(1)$, $c = 20.948(5)$ Å, $\beta = 90.16(2)°$, $V = 2823(1)$ Å^3, $Z = 8$, $D_x = 1.230$ Mg/m^3, $D_m = 1.22(2)$ Mg/m^3, Mo Kα radiation, $\lambda = 0.71069$ Å, $\mu = 0.06965$ mm^{-1}, $T = 293(2)$ K, crystal shape: irregular plate, crystal size: 0.20 mm × 0.56 mm × 0.72 mm. The unit cell dimensions were determined by least squares with 25 centered reflections for the red isoform (A) ($6.0 \le \theta \le 10.9°$) and 75 reflections for the yellow isoform (B) ($6.1° \le \theta \le 14.4°$) using graphite monochromated Mo Kα radiation. Both structures were solved by direct methods using MULTAN88 programs.[19] Atomic scattering factors for neutral atoms and dispersion corrections were used. The Xtal13.2[20] system of crystallographic programs was used for the correlation and reduction of data, structure refinement, and interpretation. ORTEPII[21] was used to produce molecular graphics, with calculations performed on VAX 8550 computers. Stereo pairs and space filling models were also generated with the Insight II V2.3.5 (Biosym Technologies, San Diego, CA) on a Silicon Graphics Extreme work station.

2-Acetyl-6-(dimethylamino)naphthalene (ADMAN, I).[5] To a solution of 5.26 g (117 mmol) of dimethylamine in 29 mL of freshly distilled hexamethylphosphoric triamide (HMPT) were added 31 mL of dry toluene and 780 mg (112 mmol) of Li in small pieces. The mixture was stirred under argon at room temperature for 1.5 h. 2-Acetyl-6-methoxynaphthalene[22] (5.57 g, 27.8 mmol) was added in one portion and stirring continued for 20 h. The mixture was cooled in an ice−water bath and poured into a cold water/ethyl acetate mixture (300 mL each). After thorough mixing, the layers were separated, and the water layer was extracted twice with 225 mL of ethyl acetate. Organic extracts were combined, dried, and evaporated to give a yellow solid. Recrystallization from ethanol afforded 3.67 g (64%) of a yellow solid, melting at 153.5−155 °C: ^{1}H NMR ($CDCl_3$, TMS) δ 2.67 (s, 3H, $COCH_3$), 3.15 (s, 6H, $N(CH_3)_2$), 6.87 (d, 1H, H-5), 7.17 (dd, 1H, H-7), 7.63 (d, 1H, H-4), 7.80 (d, 1H, H-8), 7.92 (dd, 1H, H-3), 8.32 (bs, 1H, H-1). $J_{1,3} = 2.3$ Hz, $J_{3,4} = 8.7$ Hz, $J_{5,7} = 2.4$ Hz, $J_{7,8} = 9.3$ Hz. MS (M^+) 213; found: 213. Anal. Calcd for $C_{14}H_{15}NO$: C, 78.84; H, 7.09; N, 6.57. Found: C, 78.96; H, 7.10; N, 6.45.

1,1-Dicyano-2-[6-(dimethylamino)naphthalen-2-yl]propene (DDNP, II). A mixture of malononitrile (436 mg, 6.6 mmol) and 2-acetyl-6-(dimethylamino)naphthalene (ADMAN, **I**) (1.278 g, 6 mmol) was heated to 110 °C in 20 mL of pyridine for 19 h. After cooling, the remaining red solid was dissolved in 100 mL of methylene chloride, adsorbed onto 10 g of flash silica gel (230−400 mesh) and chromatographed with toluene. Appropriate fractions were combined and evaporated to give 1.12 g (72%) of **II**. Recrystallization from benzene−hexane gave red needles melting at 154.5−155 °C: ^{1}H NMR ($CDCl_3$, TMS) δ 2.69 (s, 3H, CH_3), 3.11 (s, 6H, $N(CH_3)_2$), 6.85 (d, 1H, H-5), 7.18 (dd, 1H, H-7), 7.56 (dd, 1H, H-3), 7.66 (d, 1H, H-4), 7.76 (d, 1H, H-8), 8.02 (d, 1H, H-1). $J_{1,3} = 2.04$ Hz, $J_{3,4} = 9.13$ Hz, $J_{5,7} = 2.5$ Hz, $J_{7,8} = 9.11$ Hz. IR ($CHCl_3$) 2250 cm^{-1} (CN stretching). MS (M^+): 261; found: 261. Anal. Calcd for $C_{17}H_{15}N_3$: C, 78.13; H, 5.79; N, 18.08. Found: C, 78.17; H, 5.68; N, 17.91.

Results

Chemistry. Standard conditions described in the literature for the Knoevenagel condensation of malononitrile with substituted acetophenones[23] were not successful with **II**. Recently described conditions employing $TiCl_4$ as a catalyst could not be used with acetophenone because of side reactions.[24] Reaction in benzene or toluene with a piperidinium acetate catalyst and azeotropic removal of water gave only low conversion to the desired adduct after 12 h at reflux. Pyridine has long been known to catalyze the dehydration of the initial addition product in the Knoevenagel condensation and has been used in conjunction with secondary amines to accelerate the reaction. It was found that reaction of **I** with 1.05 equiv of malononitrile in pyridine at reflux gave a 66−85% yield of the adduct, **II**. The product was easily identified by TLC as a visible orange spot of higher R_f than the starting ketone (solvent, 100% benzene, silica gel). The compound appeared as a red solid after flash chromatography. The structure of **II** is consistent with its spectral properties.

Analytical samples of DDNP are shelf-stable at room temperature. Methanolic solutions of **II** were found to be stable for several weeks, as determined by their single emission peak at 610 nm upon excitation at either 340 or 420 nm. On the other hand, **II** slowly decomposed in other solvents (i.e., CH_3CN and ether containing solvents) giving rise to a second pair of excitation and emission bands at shorter wavelengths. The observed second fluorescent transition was found to be solvent polarity dependent, resembling the fluorescence properties of the acetyl precursor, ADMAN (**I**) (Table 1). Verification of this decomposition was obtained by HPLC analysis, wherein the decomposition product eluted as a single peak when coinjected with a purified sample of **I** (DDNP: $R_t = 9.02$ min; **I** and decomposition product of **II**: $R_t = 12.56$ min). Using this technique, the $t_{1/2}$ of decomposition of **II** in CH_3CN at 20 °C was determined to be approximately 36 days.

Electronic Absorption Spectroscopy. Substantial differences exist between the electronic absorption spectra of DDNP (**II**) and those of the parent **I**. The ultraviolet absorption maximum exhibited by the acetyl derivative **I**, centered at 360 nm ($\epsilon = 1.8 \times 10^4$), is red-shifted by 50−80 nm in the product

(14) Melhuish, W. H. *J. Opt. Soc. Am.* **1964**, *54*, 183−186.
(15) Chen, R. F. *Anal. Biochem.* **1967**, *19*, 374−387.
(16) Schnerzel, R. E.; Klosterman, N. E. *NBS Special Publication* **1976**, *526*, 3−4.
(17) Drexhage, K. N. *NBS Special Publication* **1977**, *466*, 33−40.
(18) Karstens, T.; Kobs, K. *J. Phys. Chem.* **1980**, *84*, 1871−1872.
(19) Debaerdemaeker, T.; Germain, G.; Main, P.; Refaat, L. S.; Tate, C.; Woolfson, M. M. *MULTAN88*: A System of Computer Programs for the Automatic Solutions of Crystal Structures from X-ray Diffraction Data; University of York: England, 1988.
(20) Hall, S. R.; Stewart, J. M. The Xtal3.0 system; University of Western Australia: Australia, and University of Maryland: U.S.A., 1990.
(21) Johnson, C. K. *ORTEPII*. Report ORNL-3794; Oak Ridge National Laboratory: Oak Ridge, Tennessee, 1976.
(22) Arsenijevic, L.; Arsenijevic, V.; Horeau, A.; Jacques, J. *Org. Synth. Coll.* **1988**, *6*, 34−36.
(23) Coligny, T. H.; Normant, C. R. *Acad. Sci. Paris* **1971**, *272C*, 1425−1430.
(24) Lehnert, W. *Tetrahedron* **1972**, *28*, 663−666.

Table 1. DDNP, ADMAN Electronic Absorption, and Fluorescence Data[a]

		absorption maxima (nm)		$\epsilon(1 \times 10^{-4})$		excitation maxima (nm)		emission maxima (nm)		quantum yields		
solvent	$E_T(30)$[b]	ADMAN	DDNP	ADMAN	DDNP	ADMAN	DDNP	ADMAN	DDNP	ADMAN	DDNP	τ DDNP (ps)
water	63.1	355	385	*c*	*c*	360	393	528	529	0.22	0.015	106
methanol	55.5	366	426	1.8	2.0	365	428	506	610	0.48	0.013	210
ethanol	51.9	363	434	1.8	2.0	365	410	498	600	0.63		302
acetonitrile	46.0	352	428	1.8	1.9	355	428	492	600	0.70	0.053	306
chloroform	41.1	358	444	1.9		360	450	436	548	0.17		
dichloromethane	39.1		438		2.0		456		560		0.028	245
cyclohexane	31.2	343	415	2.1		345		394	470	0.03		
hexane	30.9		412		2.5		410		468		0.0020	
heptadecane			421		2.5				468		0.0032	
low viscosity mineral oil			422		2.6				468		0.0082	
high viscosity mineral oil			422		2.6				468		0.0091	
γ-cyclodextrin											0.060	

[a] Absorption spectra determined at concentrations on the order of 1−5 μM. Fluorescence spectra were measured at concentrations of less than 0.1 O.D. at the excitation maxima. [b] $E_T(30)$ values from ref 25. [c] Concentration not determined.

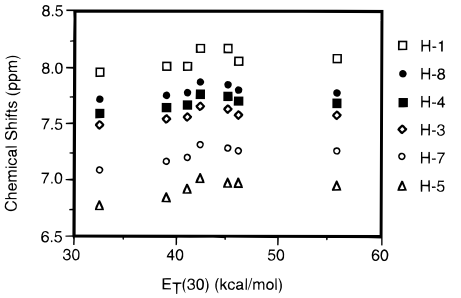

Figure 1. ^{1}H NMR chemical shifts for naphthalene protons in DDNP vs solvent $E_T(30)$ values.[25] Proton assignments were maded from single proton decoupling experiments.

of malononitrile addition. The absorption maximum of DDNP appears as a broad single transition in the 380−450 nm region, that is relatively less sensitive to solvent polarity than fluorescence excitation or emission. DDNP absorption maxima were found in the range 412 (hexane) to 444 nm (chloroform), with extinction coefficients of $\sim 2 \times 10^4$ (Table 1). Absorption maxima did not follow a simple regression but instead fell generally into an inverted "U" shaped pattern when compared by solvent polarity $E_T(30)$.[25] In investigating the ground state polarity of **II**, ^{1}H NMR spectra were determined in various solvents. Like absorption maximum, the ^{1}H chemical shifts show an inverted "U"-shaped curve when plotted against solvent polarity (Figure 1), with higher chemical shifts at intermediate solvent polarities.

Fluorescence Properties. Highly purified samples of **II** were used for absorption and fluorescence determinations. DDNP was found to be poorly fluorescent in organic and aqueous solvent media. Quantum yields varied from 4×10^{-4} to 5×10^{-2} and were considerably lower than those of **I** (Table 1). As with **I**, however, quantum yields appear highest in solvents with intermediate polarity, with lower yields in aqueous and nonpolar solvents. Emission wavelengths appear to move to successively lower energies with increasing solvent polarity, as is generally found with excited state charge transfer (CT) complexes. In water, fluorescence was anomalously blue-shifted with a significant reduction in Stokes shift (Table 1), which can be attributed to the formation of microaggregates. [The blue-shift is coincident with the fluorescent emission spectra of **I**. The fluorescence emission observed is not believed to be due to decomposition to **II** in water, however, as there was no chromatographically detectable amount of **I** in the sample tested. Moreover, the excitation spectra of the two compounds in aqueous media are dissimilar.] Addition of protein (e.g., bovine serum albumin, BSA) to aqueous solutions of **II** elicits an increase in fluorescence intensity and a hypsochromic shift of the fluorescence excitation and emission maxima (Figure 2), an effect likely due to DDNP binding to hydrophobic pockets on the protein surface. The substantial red-shift in excitation spectra with BSA addition (Figure 2, inset) is similar to changes observed in moving from water to more intermediate polarity solvents (e.g., CH_3CN) (Table 1). In order to assess the effect of viscosity, DDNP fluorescence emission spectra were measured in a series of poly(ethylene)glycols (Figure 3). Fluorescence emission intensity and relative quantum yields were found to increase strongly with increasing kinematic viscosity over the range 18−140 centiStokes. Emission wavelengths were noted to shift slightly to higher energies with increasing chain length.

As the nature of the solvent changes somewhat with increasing chain length in the ethylene glycols, experiments were conducted with a series of alkanes in order to separate the effect of changing solvent functionality from viscosity sensitivity (Figure 4). Even though fluorescence quantum yields increase 4.6-fold over a viscosity range of 0.45−156 centiStokes, no change in wavelength was observed under these conditions, confirming the absence of solvatochromatic effects with viscosity as the only changing parameter. Similarly, fluorescence intensity of the emission spectrum in glycerol at −50 °C increased three-fold over that at room temperature in the same solvent. As shown in Figure 5A, the fluorescence maximum at −50 °C is at 550 nm, reducing the Stokes shift from 6.6×10^3 to 1.1×10^2 cm^{-1} since no similar shift was observed in the excitation spectrum with temperature. The temperature itself is not an important factor in this change since the fluorescence spectrum in methanolic solution at −50 °C was instead red-shifted to 620 from 600 nm at room temperature. As expected, however, the fluorescence yield proved to be very sensitive to temperature (Figure 5B).

Solid State Properties. DDNP (**II**) was isolated in two different crystalline forms from benzene solution under petroleum ether vapor: (A) as fine red needles, formed with fast growth in concentrated solution, and (B) as yellow plates, formed slowly from dilute solution. X-ray measurements confirm that A and B are polymorphs of the same substance. Although these isoforms produce identical ^{1}H NMR, absorption, and fluorescence properties when in solution, they revealed very different fluorescent emission properties in the solid state, with the red and yellow material showing emission maxima of 645 and 580 nm, respectively (Figure 6).

The asymmetric unit of modification A contains only one

(25) Reichardt, C. Solvent Effects in Organic Chemistry; Verlag Chimie: Weinheim, 1979; pp 242−244.

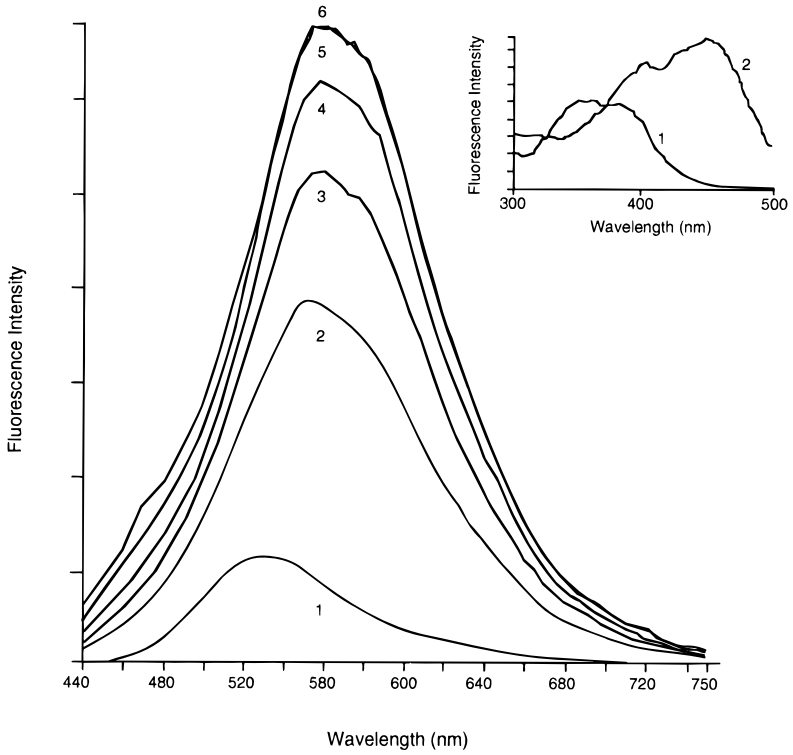

Figure 2. Corrected fluorescence emission spectra of DDNP in water with increasing concentrations of bovine serum albumin (BSA) at 20 °C: (1) water; (2) 0.5 mg/mL BSA; (3) 1 mg/mL BSA; (4) 2 mg/mL BSA; (5) 7 mg/mL BSA; (6) 11 mg/mL BSA. Higher concentration of BSA induced no additional fluorescence changes. Excitation = 420 nm. Inset shows DDNP fluorescence excitation spectra in water (1) and upon addition of BSA (1 mg/mL) (2).

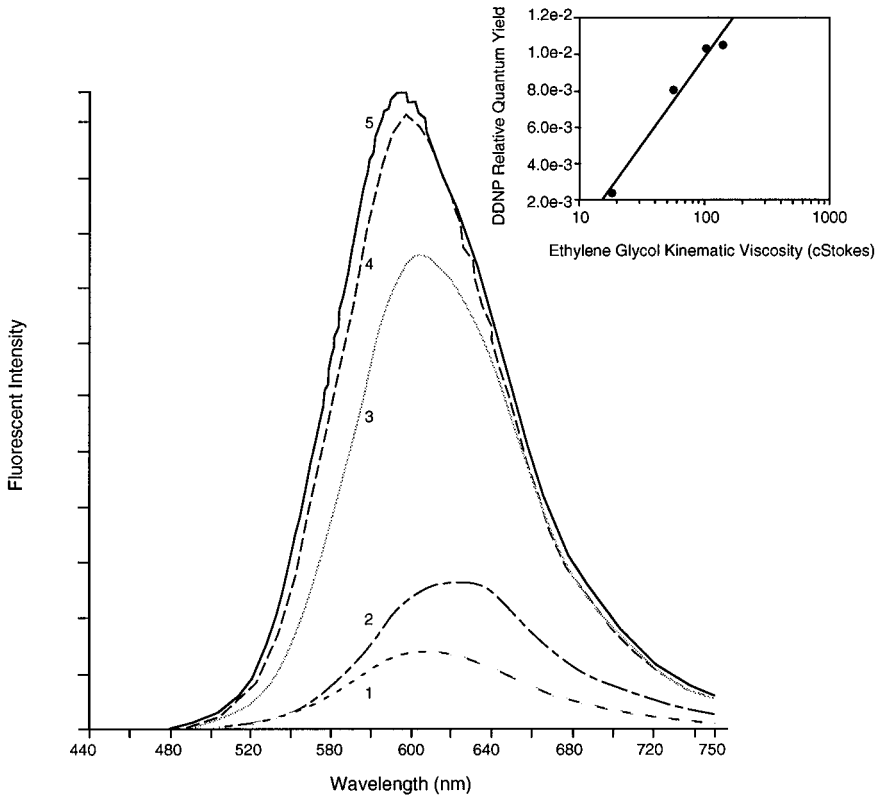

Figure 3. Corrected room temperature fluorescence emission spectra of DDNP in MeOH (1, 0.695 centiStokes), ethylene glycol (2, 18 centiStokes), and neat polyethylene glycol mixture of different viscosities (3), PEG200, 58 centiStokes, (4), PEG400, 105 centiStokes, and (5), PEG 600, 140 centiStokes. Excitation = 420 nm. Inset shows the relationship between quantum yield and viscosity in the polyethylene glycol series. Log_{10} curve fit $R^2 = 0.982$. Note: changes in fluorescence emission wavelength are probably due to changes in solvent polarities.

molecule, whereas modification B has two formula units: (a) and (b). Most bond angles of all conformers showed remarkable similarities, except for the orientation of substituent groups around the C(2)−C(11) bond (Table 2). The orientation of dihedral angles appeared to be reversed between B(a) and B(b) in the yellow solid. The malononitrile group orients toward

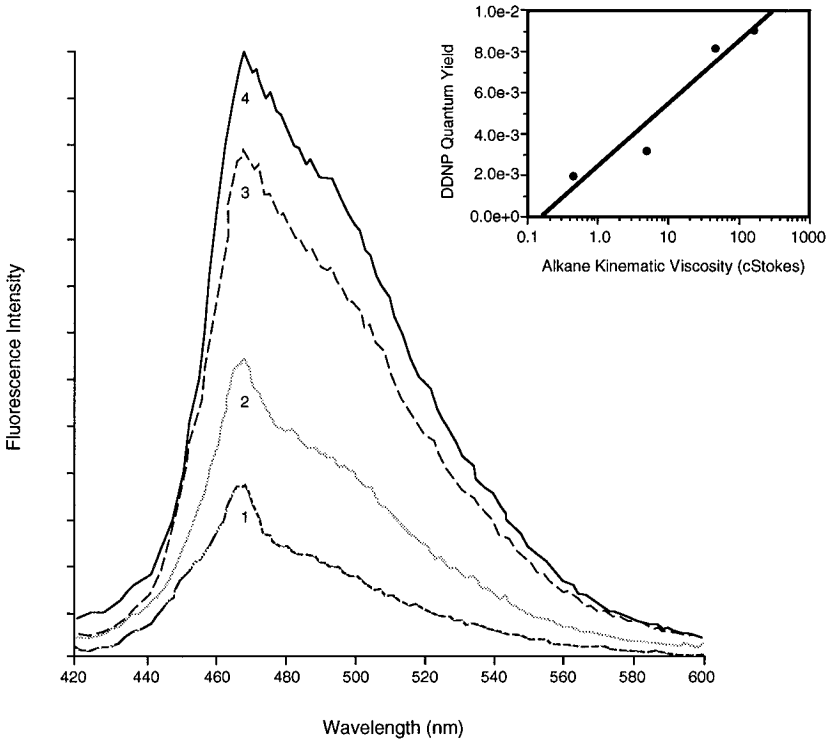

Figure 4. Corrected room temperature fluorescence emission spectra of DDNP in alkanes of different viscosities: hexane (1, 0.445 centiStokes), heptadecane (2, 4.79 centiStokes), low viscosity mineral oil (3, 45.99 centiStokes), and high viscosity mineral oil (4, 156.10 centiStokes). Inset shows the relationship between quantum yield and viscosity in this series. Log_{10} curve fit $R^2 = 0.932$.

Table 2. Selected Torsion Angles (in deg) for DDNP Crystal Isoforms (for Numbering see Figure 8)[a]

dihedral	isoform (A)	(B)(a)	(B)(b)
C1−C2−C11−C12	28.7	37.7	143.3
C1−C2−C11−C13	−152.3	−141.5	−38.0
C3−C2−C11−C12	−147.9	−140.7	−34.9
C3−C2−C11−C13	31.0	40.1	143.7
C2−C11−C13−C14	−175.1	−178.0	−179.9
C2−C11−C13−C15	9.3	1.7	−2.2
C12−C11−C13−C14	3.8	2.8	−1.2
C12−C11−C13−C15	−171.8	−177.5	176.5
C6−C7−N3−C16	179.8	0	175.1
C6−C7−N3−C17	−3.7	−173.3	−5.1
C8−C7−N3−C16	0.6	−179.5	−4.9
C8−C7−N3−C17	177.1	7.3	175.0

[a] Both isoforms crystallize in $P2_1/n$ space group, which possesses a center of symmetry. Therefore, in both solid isoforms, 50% of the molecules have the torsion angles listed above, and the other 50% have the same absolute values but with opposite sign.

carbon-3 in B(a) (dihedral C(1)−C(2)−C(11)−C(13) = 37.9°) or carbon-1 in B(b) (dihedral C(1)−C(2)−C(11)−C(13) = 143.3°) in the naphthalene ring. The orientation of the malononitrile group in A (red modification) is similar to that of B(a), but with smaller C(1)−C(2)−C(11)−C(13) torsion angle (28.7°) (Figure 7). In all three conformers, the dimethylamino moiety is close to planar with the naphthalene ring (±0−7° rotation, Table 2). Bond lengths are similar in all three forms and correspond to the expected values. The shortest intermolecular contact in (A) is 3.56(1) Å between C(12) and N(2)$^{(i)}$ ((i): 3/2−x, 1/2+y, 1/2−z), and in (B) 3.27(1) Å between N(1b) and N(1b)$^{(ii)}$ of two symmetry related molecules ((ii): −x, 1 − y, −z). Significant aromatic ring overlap (vertical stacking) exists in the yellow form between the two conformers (Figure 8).

Labeling Applications. A functional example of the utility of DDNP environmental sensitivity was demonstrated in its application as a general cell stain in confocal imaging of live Ltk$^-$ mouse fibroblast cells (Figure 9). With DDNP staining, intense fluorescence was observed with cell membranes and internal structures (488 nm illumination and emission above 525 nm). With the fluorophore applied in concentrations ranging from 50 nM to 10 μM, with 20−30 s exposure prior to imaging, no increase in background signal was observed. These cells could be imaged for several hours when kept alive in growth medium, with little or no photobleaching or other loss in signal strength.

Discussion

The fluorescence probe 1,1-dicyano-2-[6-(dimethylamino)-naphthalen-2-yl]propene (**II**, DDNP) was developed as a neutral, lipophilic probe for use with fluorescence spectroscopy. Because **II** is uncharged at physiological pH, it can cross membrane barriers, and when linked to a molecule of biological interest, it can be used to study intracellular *in vivo* processes. When used with an argon ion or argon/krypton laser source, a probe for fluorescence microscopy should have significant excitation at 488 nm and a large enough Stokes shift to filter appropriately excitation from emission wavelengths. Indeed, **II** exhibits an intense absorption band in the visible region (Table 1). The long wavelength $S_0 \rightarrow S_1$ absorption band was observed to move to generally lower energies with increasing solvent polarity, with the exception of water where DDNP absorption was found to be strongly blue-shifted. Increases in absorption band-width were also observed with increasing solvent polarity. Fluorescence emission spectra ($S_1 \rightarrow S_0$) exhibited the same sensitivity to solvent polarity (Table 1) demonstrating the highly polar nature of the S_1 excited state. The long wavelength fluorescence emission of DDNP observed in more polar solvents is undoubtedly due to an intramolecular $\pi^* \rightarrow \pi$[26] charge transfer (CT) transition. A question can be raised, however, as to whether DDNP fluorescence observed in solvent systems is due to

(26) Lippert, E.; Luder, W.; Boos, H. Advances in Molecular Spectroscopy; Mangini, A., Ed.; Pergamon Press: Oxford, 1962; p 443.

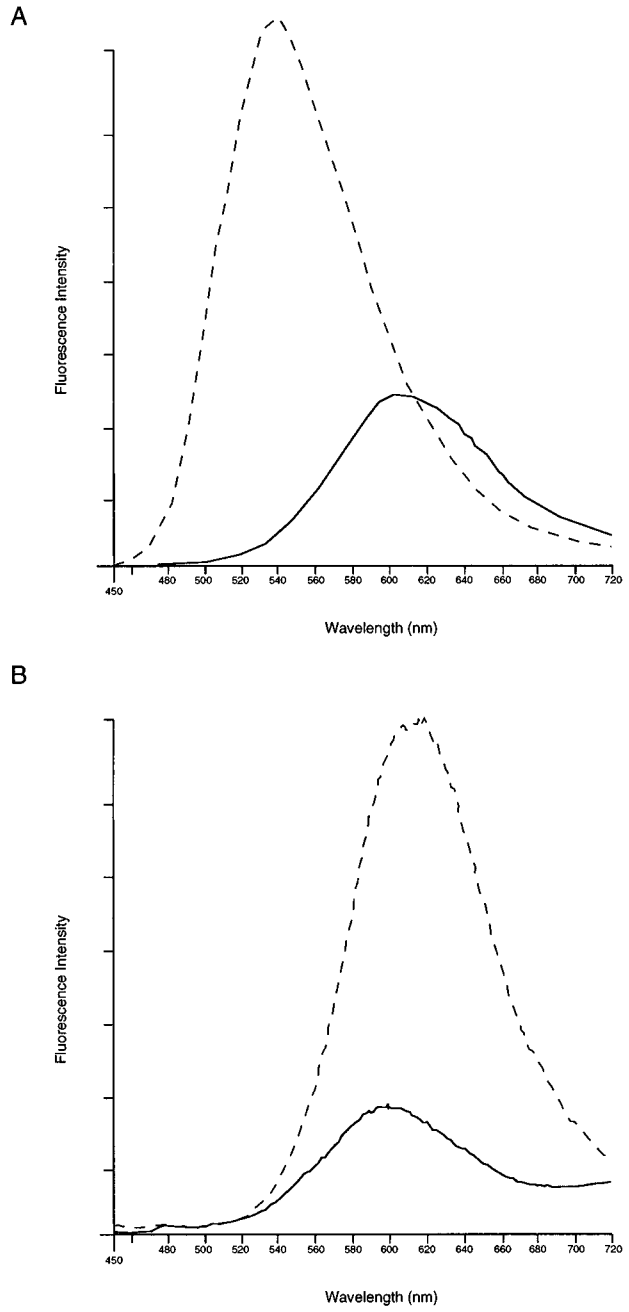

Figure 5. A. Molecule fluorescence emission spectra of DDNP in glycerol at room temperature (—) and glycerol at −50% (− − −); B, in methanol at room temperature (—) and methanol at −50° (− − −). Excitation at 460 nm.

emission from planar or "twisted" charge transfer states.[10] Although we have not yet attempted to determine orientation in solvent systems, a number of features of the fluorescent properties of the solid state structure reflect on the importance of the orientation of donor and acceptor substituents to the π system.

The peak of fluorescence emission in the yellow solid (B(a) and B(b)) is somewhat bathochromically shifted from that of the red form (A), suggesting an increased energy of the prominent CT transition. The lesser twisting in the longer wavelength (red) fluorescent form of the solid would seem to raise the possibility that a more planar, "biradical" or biradicaloid" CT[27,28] transition is of the lowest energy in this system.

(27) Bonačić-Koutecký, V.; Michl, J. *J. Am. Chem. Soc.* **1985**, *107*, 1765−1766.

(28) Nowak, W.; Rettig, W. *J. Mol. Struct. (Theochem)* **1993**, *102*, 1−12.

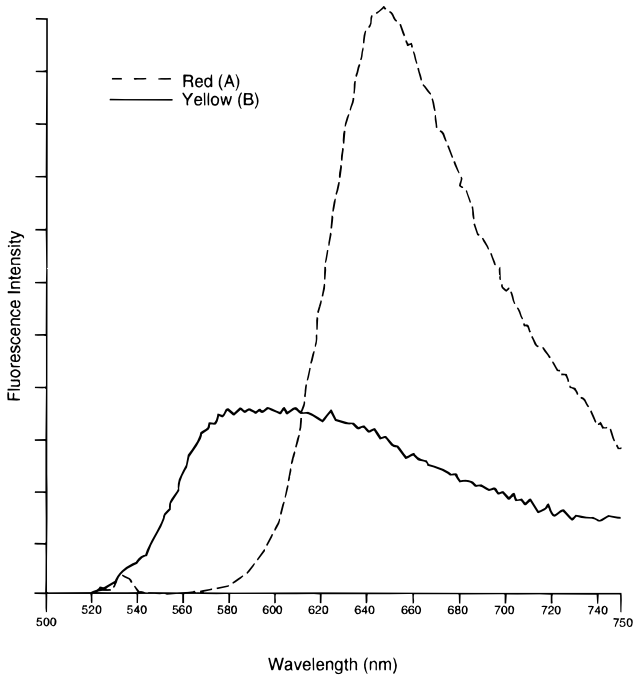

Figure 6. Corrected fluorescence emission spectra for the red (A) and yellow (B) isoforms of DDNP.

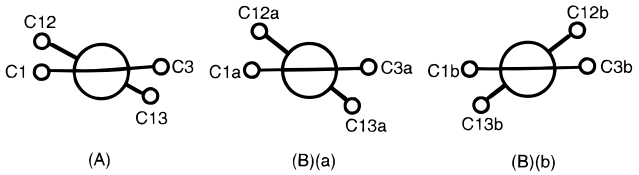

Figure 7. Newman projections of parts of molecules of (A) and (B), looking in the C(2)−C(11) direction.

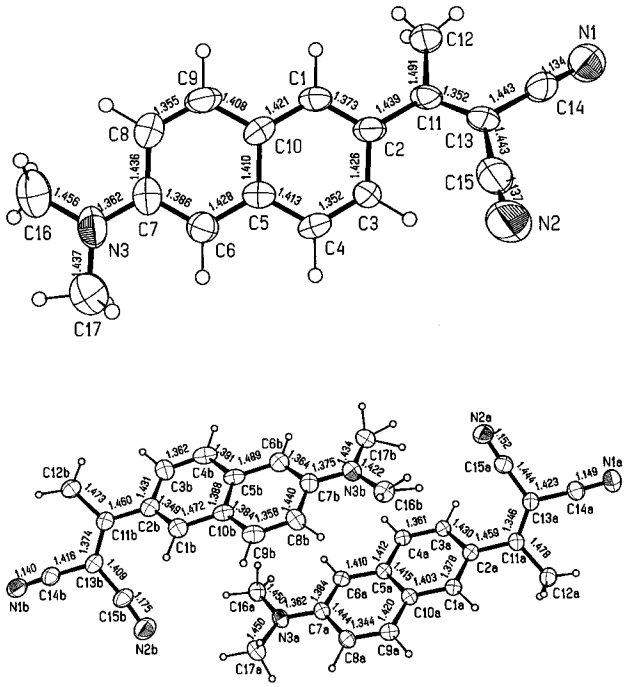

Figure 8. ORTEP representations of DDNP red (A) and yellow (B) crystal isoforms with position and bond lengths shown.

In that the yellow crystal form reveals an extremely broad emission, it is likely that the observed fluorescence is a composite of emission from the two conformers (B(a) and B(b)) present in the crystal. On the other hand, while the difference in planarity of malononitrile groups is notable, it would appear

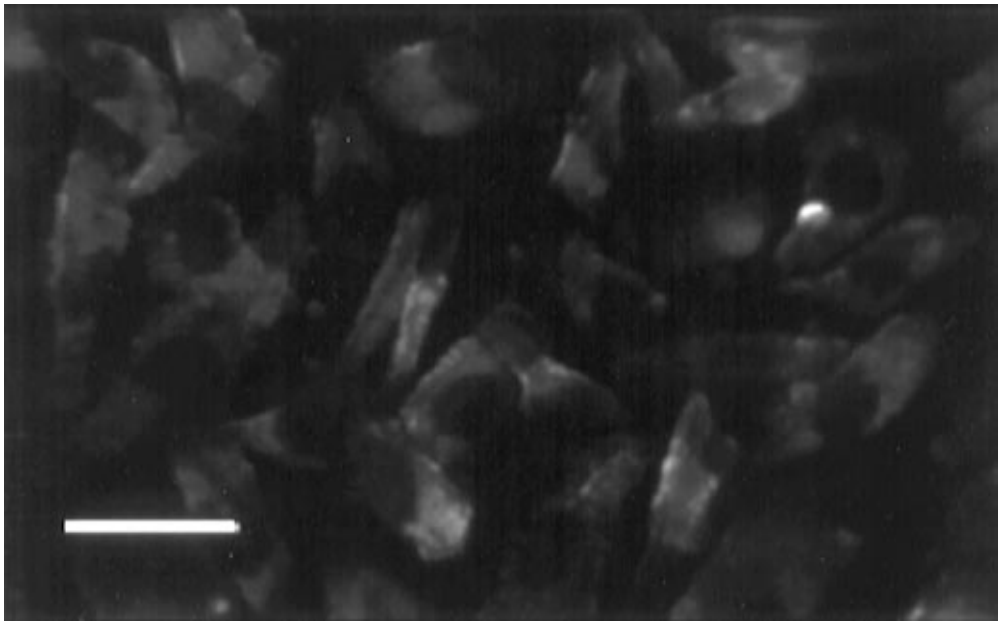

Figure 9. Cultured Ltk-mouse fibroblast cells stained with 500 nM DDNP. Image generated on BioRad MRC 600 confocal fluorescent scanning microscope. Excitation = 488 nm, argon ion laser. Emission above 525 nm. Scale bar is 25 μm.

unlikely that only differences in torsion angle would account for the approximate 80 nm red shift in fluorescence maxima between the two crystal forms. This large wavelength change may require much larger changes in the geometry or conjugation of the molecule, a factor that may be provided by the intermolecular effects of stacking in the crystal. In the yellow form there are two conformers of DDNP stacked in close proximity in a head to toe fashion, whereas in the red form very little overlap exists between the molecules (Figure 8). From the overlap and closeness of the ring systems of the yellow form, it would appear that significant $\pi-\pi$ stacking may occur. This raises the possibility that, along with the out-of-plane rotation of the malononitrile group, intermolecular electronic (excimer) effects may participate in the broadening and bathochromic shift of fluorescence maxima.

Clearly, our solid state fluorescence data have limited quantitative significance but offer direct evidence that fluorescence emission in DDNP originates in out-of-plane conformers. The dihedral angle (θ) between the naphthalene ring and the malononitrile moieties in the crystal structure for all conformers found (A, red; B(a), B(b), yellow) departs significantly from zero. Although our findings of approximate planarity between dimethylamino and naphthalene moieties in both crystal species are consistent with previous reports of PRODAN crystal structure,[29] the observation of long wavelength CT emission would appear to contrast with the general view of intramolecular charge transfer states in highly extended donor−aryl−acceptor systems.[9−12,29−35] Modeling of electronic transitions in these systems has generally ascribed long wavelength fluorescence to twisted intramolecular CT, with the dialkylamino electron donor group perpendicular to the ring system plane in the excited state. Though dual fluorescence may occur in solution from both planar and twisted conformations of the dimethylamino moiety in DDNP or with interconversion between states, the crystal structures presented here demonstrate conclusively that a twisted donor-ring structure, with complete charge separation, is not a necessity to produce the long wavelength emission. In this system, the significant dihedral angle between the aromatic ring and the electron acceptor moiety (malononitrile) may produce effective charge separation to effect low energy solvatochromatic emission sensitivity.

The fluorescence quantum yield of **II** is low in most solvents but is found to increase with solvent viscosity (Figures 3 and 4) suggesting that the π^* CT excited state is greatly depopulated during the fluorescent lifetime by internal conversion within the molecule. By analogy with similar systems, this S_1 state relaxation most likely occurs by photoisomerization around the propene double bond.[36] In comparison with the isomerization and twisting of the C═C bond in *trans*-stilbene, wherein the rate is estimated at $\sim 1 \times 10^{10}$ s^{-1},[37] rotation around the ethylene bond in **II** is expected to be much greater considering the large difference in electronegativity of substituent groups across the bond.[38] By contrast, fluorescence deexcitation of **II** is unlikely to occur by torsion of the donor or acceptor groups from the naphthalene plane. The rotation rates in the ground state of the malononitrile and dialkyl amino groups in [*p*-*N*,*N*-dialkylaminobenzylidene]malononitriles have been reported to be approximately 5×10^4 and 1×10^7 s^{-1}, respectively.[39] In the excited state these rotations are expected to be yet slower due to the attainment of partial double bond character and are essentially frozen during the fluorescent lifetime.[40] Rotation of these groups thus cannot account for the low quantum yield of **II**.

Taken together, these data suggest that the very low fluorescence yield of **II** in nonviscous solvents is the result of a fast nonradiative deactivation of the singlet excited state

(29) Ilich, P.; Pendergast, F. G. *J. Phys. Chem.* **1989**, *93*, 4441−4447.
(30) Grabowski, Z. R.; Rotkiewicz, K.; Siemiarczuk, A.; Cowley, D. J.; Baumann, W. *Nouv. J. Chim.* **1979**, *3*, 443−454.
(31) Rotkiewicz, K.; Grellman, K. H.; Grabowski, Z. R. *Chem. Phys. Lett.* **1973**, *19*, 315−318; *erratum* **1973**, *21*, 212.
(32) Rettig, W.; Bonačić-Koutecký, V. *Chem. Phys. Lett.* **1979**, *62*, 115−120.
(33) Lipinski, J.; Chojnacki, H.; Grabowski, Z. R.; Rotkiewicz, K. *Chem. Phys. Lett.* **1980**, *70*, 449−453.
(34) Grabowski, Z. R.; Dobkowski, J.; Kühnle, W. *J. Mol. Struct.* **1984**, *114*, 93−100.
(35) Rulliere, C.; Grabowski, Z. R.; Dobkowski, J. *Chem. Phys. Lett.* **1987**, *137*, 408−413.
(36) Safarzadeh-Amiri, A. *Chem. Phys. Lett.* **1986**, *129*, 225−230.
(37) Greene, B. I.; Hochstrasser, R. M.; Weisman, R. B. *J. Chem. Phys.* **1979**, *71*, 544−545.
(38) Bonačić-Koutecký, V.; Köhler, J.; Michl, J. *Chem. Phys. Lett.* **1984**, *104*, 440−443.
(39) Safarzadeh-Amiri, A. *Can. J. Chem.* **1984**, *62*, 1895−1898.
(40) Porter, G.; Suppan, P. *Trans. Faraday Soc.* **1965**, *61*, 1664−1673.

associated with C(11)−C(13) double bond isomerization. Internal rotational relaxation of the bond that connects the naphthalene ring and the dicyanopropylene group would produce conformers susceptible to fluorescence deactivation[36] in the excited state. Restrictions placed on C(11)−C(13) double bond isomerization with increased probability of intramolecular rotation around the donor−acceptor C(2)−C(11) bond may additionally be responsible for the environmental sensitivity of **II** to protein binding. Addition of bovine serum albumin (BSA) to DDNP in aqueous solutions results in over six-fold increase in fluorescence intensity, a complete shift in excitation wavelength, from 393 nm to 464 nm, and a concomitant shift in emission wavelength, from 530 nm to 570 nm (Figure 2). Therefore, in the presence of proteins any contribution to the fluorescent signal from the unbound fluorophore is negligible compared with the emission of the probe bound to the macromolecule. This constitutes a highly desirable property for fluorescence microscopy. Similarly, the same rotor effect[39,41] can be used to explain the rigidity dependence (i.e., with γ-cyclodextrin) and the viscosity effects[3] observed when the fluorescence emission properties are determined in glycol or alkane series at room temperature or with glycerol at −50 °C, where quantum yields are found to increase dramatically with increased kinematic viscosity (Figures 3−5).

Because of the strong visible wavelength solvatochromatism and viscosity sensitivity, DDNP appears to be a highly useful probe for biological assays. As DDNP is hydrophobic, and uncharged at physiological pH, it is able to readily pass cell membranes and, if conjugated with a pharmacological agent, could be used to study a variety of intracellular processes *in vivo*. To separate in cell labeling experiments the contributions of viscosity and polarity to fluorescence emission would be difficult. However, this limitation should not detract from the use of DDNP in biological experiments. Unlike the UV fluorescent compound PRODAN, a broad long wavelength excitation spectra in protein and intermediate polarity solvent media is found for DDNP, allowing its use with 488 nm illumination from the argon ion, or argon/krypton lasers commonly used in visible wavelength fluorescent confocal microscopy, or conventional fluorescence microscopy using a lamp source.

The intensity of emission at submicromolar concentrations of DDNP, with very short ligand exposure time, demonstrates its high efficacy for protein and membrane labeling. The rapid labeling of internal components suggests rapid diffusion of **II** through membranes. Moreover, a negligible signal from DDNP in unbound state in the cytosol (or bathing media) adds a unique advantage in its combination of solvent polarity and viscosity sensitivity in the visible wavelength range with low background signal. Conjugation of this probe to high affinity ligands for investigating *in vivo* biochemical processes (e.g., receptor binding and modulation) increases its range of applicability. This work will be published elsewhere.

Acknowledgment. This work was supported in part by Department of Energy Grant DE-FC0387-ER60615 and in part by the Ministry of Science and Technology of the Republic of Slovenia (travel expenses for A.P.). Special thanks are given to Professor G. Weber for valuable discussions and determination of fluorescence lifetimes.

(41) Kung, C. E.; Reed, J. K. *Biochemistry* **1989**, *28*, 6678−6686.

JA9543356